Blunt Body Pitch Damping Measurements from Multiple Subsonic Free-to-Pitch Magnetic Suspension Trials

Mark Schoenenberger[1], David Cox[1] and Colin Britcher[2]
[1] NASA Langley Research Center
Hampton, Virginia 23681, USA
[2] Old Dominion University
Norfolk, Virginia 23529, USA

ABSTRACT

The yaw damping coefficients of two blunt entry vehicle models, measured from free-to-oscillate tests in the ODU/NASA subsonic magnetic suspension wind tunnel are presented. Multiple repeat trials were conducted for both models. Two separate data reduction methods were used to extract damping coefficients and yaw moment slope. Both methods identified similar damping and stability values, with differences being consistent with their known limitations.

1. Introduction

The MIT/ODU/NASA subsonic magnetic suspension wind tunnel has been configured for free-to-oscillate pitch damping tests of blunt body entry vehicles. Early trials have shown that yaw moment stability and yaw damping coefficients can be extracted from camera position and orientation tracking [1]. Preliminary uncertainty analysis indicated that magnetic control inputs were not a large contributor to overall uncertainty of the extracted parameters [2]. This work continues those preliminary studies with multiple trials to better assess the repeatability of the measured parameters. Two different models were tested and two different data reduction techniques were utilized with data from tests of both shapes. The Earth Entry Vehicle (EEV) is representative of candidate shapes being considered for a Mars sample return mission. The Stardust entry vehicle is a capsule that returned samples a comet tail in 2006 [3]. The dimensions of the models tested are provided in Figure 1. Note that the structure forming the aerodynamic surfaces were made of 3D printed plastic holding 19.05mm diameter by 19.05mm length neodymium magnet cores. As the magnet core of the EEV model comprised an axisymmetric part of the outer mold line, it was magnetized with the north and south poles normal to the symmetry axis, while the Stardust core was magnetized along its axis but installed transverse to the vehicle spin axis. Both models were therefore free-to-yaw when levitated in the tunnel.

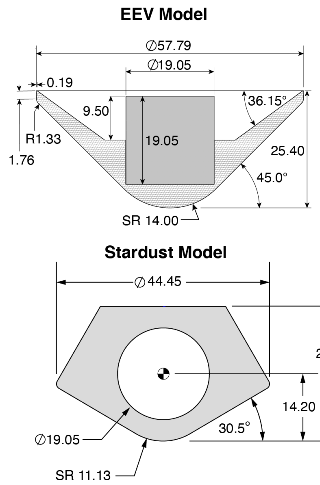

Symbol	Definition
A	amplitude constant
C_{L_β}	lift slope coeff.
C_{MAG}	magnetic coeff.
C_{n_r}	yaw damping coeff.
C_{n_β}	yaw static stability
d	ref. diameter
I	moment of inertia
m	mass
S	ref. area
t	time
V	velocity
ρ	air density
β	sideslip angle
ϕ	phase shift

Fig. 1: Model geometries (dimensions in mm) and nomenclature

2. Wind Tunnel Testing

The MIT/NASA/ODU subsonic tunnel was originally designed with axial magnetization and full 6-DoF control in the late 1960s. For our modern application, power to the MSBS coils was reconfigured and a new control algorithm was implemented to produce a vertical magnetizing field and position control only [4]. This configuration allows the levitation of models with low-aspect ratio permanent magnet cores, with or without 3D-printed plastic shells forming a desired aerodynamic shape.

Corresponding author: Mark Schoenenberger
E-mail address: mark.schoenenberger@nasa.gov

The spherical or cylindrical magnet cores are levitated and align with the vertical bias field creating a near frictionless bearing, permitting free yaw motion of the model. A pneumatically retractible support sting holds the test model at a desired initial attitude, before quickly retracting for the model to oscillate about the vertical axis. A high speed camera recorded the model motion and tracking dots were used to measure the capsule attitude versus time. The retractible sting can be brought forward to arrest capsule motion and perform repeat runs without shutting down the tunnel. In this fashion multiple runs of about four seconds can be capture on video in just a few minutes for later post-processing and data reduction. For this work, aerodynamic parameters extracted from eight Stardust trials and nine EEV trials are presented. Dynamic pressure varied between 46 and 152 Pascals. The freestream density was equal to ambient density, near sea level (1.225 kg/m^3).

Typically free-to-pitch dynamic stability testing identifies a pitch damping coefficient. For the our subsonic MSBS tunnel, the oscillation degree of freedom is in the yaw direction (the vehicle nose is free to rotate to the left and right) relative to a viewer standing next to the tunnel observing the test. To avoid inconsistency with the coordinate frames of the tunnel, the equations of motion and data reduction methods are formulated to describe yawing oscillations and extract yaw stability and damping.

3. Harmonic Oscillator Data Reduction

Assuming constant flow conditions and linear aerodynamics, including a constant damping coefficient over the range of oscillations observed, the capsule motion can be described is a simple harmonic oscillator (SHO) with an analytic solution describing the angle-of-sideslip history

$$\begin{aligned}\beta &= Ae^{\frac{\rho VS}{4m}\left(C_{L_\beta}+C_{MAG}+\frac{md^2}{2I}C_{n_r}\right)t} \\ &\quad \cos\left(\sqrt{\left(\frac{\rho V^2 Sd}{2I}C_{n_\beta}\right)}t+\phi\right)\end{aligned} \tag{1}$$

The exponent in Equation 1 describes the capsule amplitude growth or decay while the cosine term describes the oscillation frequency. The frequency is driven by the yaw static stability (as well as freestream conditions and model geometry and mass parameters). The oscillation growth or decay is driven by the yaw damping as well as the lift curve slope and transverse magnetic forces. As the magnetic forces are produced from an active control system responding capsule motion, they are not easily described in this simple planar model. The term C_{MAG} was added to the analytic solution to represent the effective contribution to capsule growth and decay from the magnetic forces of the MSBS. This parameter must be estimated a priori using a full 6-DoF simulation of the magnetic suspension wind tunnel. For this approach, the lift curve slope is also provided a priori from static wind tunnel test data. With these assumed parameters, the yaw damping can be determined by fitting this equation to the raw attitude data measured by camera. Examples of these curve fits are shown in Figures 2 and 3.

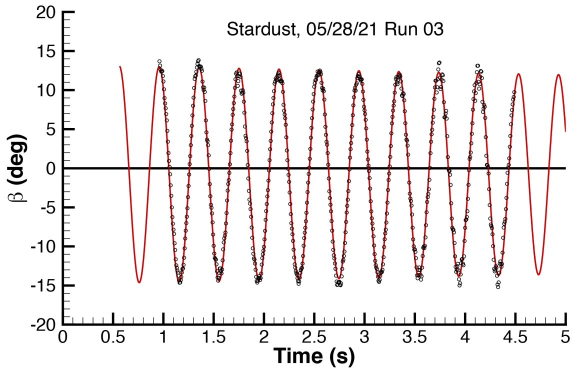

Fig. 2: SHO curve fit through Stardust trial 03

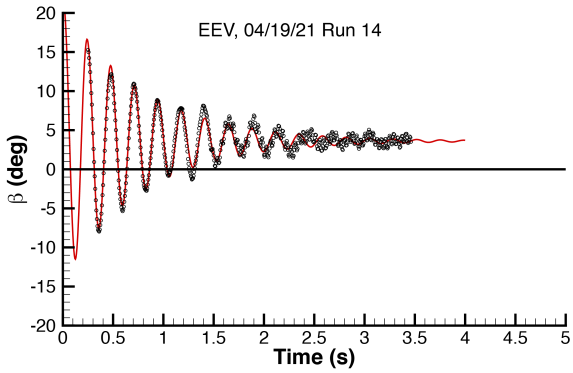

Fig. 3: SHO curve fit through EEV trial 14

Uncertainty analysis by McKown [2] determined that this data reduction method was a robust approach and the approximations made, using a priori estimates for lift and magnetic forces did not introduce large errors in the measured damping or static stability parameters. That uncertainty analysis did not look at the variations from multiple repeats. The scatter from multiple repeats are presented in Section 5..

4. System Parameter Identification

To improve upon the SHO curve fitting method, a higher fidelity data reduction method was developed that uses a dynamic-tare for removal of the magnetic suspension forces and identifies the aerodynamic forces and moments. First, a transfer function model for the magnetic system is identified with the tunnel in a wind-off state. Then a second response is obtained with the suspended model under flow conditions. The portion of the flow response which cannot be explained by the magnetic suspension forces is attributed to aerodynamic coefficients. This method has the benefit of empirically characterizing the MSBS contribution to capsule motion, where the SHO curve fit method must approximate the contribution using a pretest simulation.

The magnetic suspension model was reduced to two dimensions, plunge motion across the flow direction and a yaw motion about the magnetization vector. The force to plunge response was empirically modeled with a 4th order transfer function. Using an external input to the suspension coils a calibrated side force was applied to the model and it's plunge motion recorded. A sine-sweep profile was chosen to provide broadband excitation data, ensuring it covers the range of oscillations expected under flow conditions. This model was augmented with rotational dynamics, based only on the models inertia, with an input as the cg-referenced torque. The result is a dynamic model for the system with no-flow, with inputs of side-force and yaw torque.

Under flow conditions the model was released from an initial yaw angle and the response recorded using both a camera system for rotation and the Electromagnetic Position Sensor (EPS) system for position. A parametric linear model was built which considers the aerodynamic stiffness, C_{N_β} , yaw damping, C_{n_r} , and lift slope, C_{L_β}. These act as feedback around the magnetic suspension model, producing forces and torques proportional to sideslip and yaw rate. An optimization problem was posed, using the Matlab's System Identification routines, to solve for the aero coefficients that minimized errors in the predicting the initial condition response under flow conditions.

A comparison of the parameter identification fit through the raw yaw and slip histories of Stardust trial 05 is shown in Figure 4. Unlike the simple analytic solution used in the SHO-fit method, the parameter identification method fits a full reconstruction of the model attitude and motion using the magnet system response model and the reconstructed aerodynamics force and moment coefficients. This method finds a better fit through the full run history including initial position drift upon release from the support sting. This method provides a higher fidelity reconstruction than the SHO-fit method, with the ability to separate MSBS and aerodynamic contributions to model dynamics, using a system response model determined experimentally.

5. Results and Discussion

The aero coefficients identified using the SHO-fit methods are shown here, EEV data in Figure 1 and Stardust in Figure 2. Both models identified a very consistent yaw stability coefficient from run to run. The frequency of oscillation in each trial was very consistent and the cosine term in the analytic solution was well suited to extract the frequencies. The damping coefficients are more scattered, but cluster around a consistent result for both models. EEV is dynamically stable, while the Stardust model is close to neutrally stable. The assumed magnet force corrections terms (determined from 6-DoF simulation and lift curve slope (from static wind tunnel test) are given in the table titles for reference.

The aero solutions obtained using the Parameter ID method for repeat runs and different flow conditions are shown for the EEV model in Table 3 and the Stardust model in Ta-

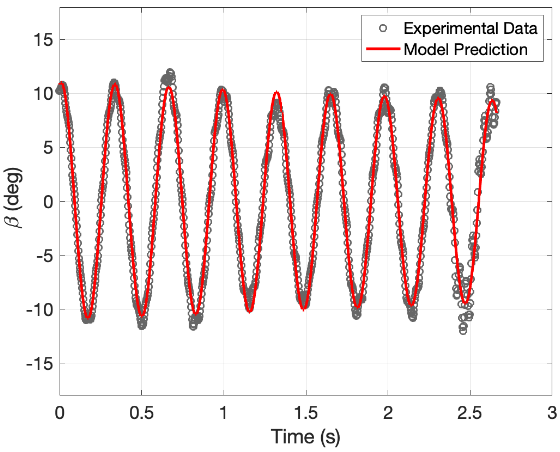

(a) Yaw oscillation history

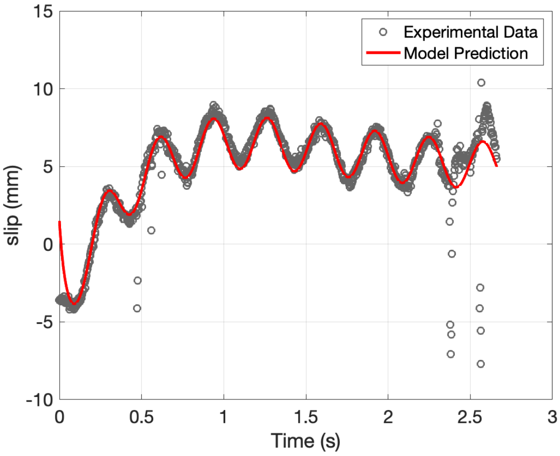

(b) Transverse (slip) motion history

Fig. 4: Parameter ID fits for Stardust Trial 06

ble 4. The estimate is very consistent for C_{n_β} as this parameter determines the frequency of the response, and small frequency errors give rise to large prediction errors. The C_{n_β} values determied from the two different methods are in very good agreement.

The damping term, C_{n_r}, is also well fit to the response, but more run-to-run variability exists here in the response data. The lift term, C_{L_β}, has the least coupling to the response data, and is therefore the most difficult to fit consistently. If the controller is aggressive enough in centering the model then aero driven plunge motion can be lost in the closed-loop response. This is one of the areas where the controller design can be tailored to ensure it allows plunge oscillations driven from the aerodynamic forcing, but still imparts sufficient centering forces to provide a robust suspension. Note that due to the forebody shape of the EEV model, the lift slope is fairly shallow and therefore produced very little plunge motion. For EEV, a lift curve slope of 0.224 was assumed, based on static subsonic wind tunnel data from an prior test. The more blunt Stardust capsule has a signicantly steeper lift curve. Tests runs observed significant plunging motion from which the Parameter ID method could find a good solution for the lift curve slope. Refer back to the plot of the fit to slip data in Figure 4.

Table 1: EEV SHO-Fit Results, $C_{MAG} = -0.244$, $C_{L_\beta} = 0.24$

Run	q (Pa)	C_{n_β}	C_{n_r}
07	43.7	0.191	-0.243
08	43.7	0.186	-0.280
09	43.9	0.186	-0.349
10	43.7	0.189	-0.372
11	96.4	0.185	-0.188
12	95.8	0.187	-0.225
13	95.9	0.185	-0.240
14	95.8	0.192	-0.295

Table 2: Stardust SHO-Fit Results, $C_{MAG} = -1.237$, $C_{L_\beta} = 0.85$

Run	q (Pa)	C_{n_β}	C_{n_r}
02	105.2	0.125	-0.035
03	104.7	0.125	0.006
04	104.8	0.123	0.096
05	104.0	0.122	-0.115
06	152.7	0.126	-0.018
07	153.2	0.127	0.027
08	153.2	0.125	0.004
12	148.9	0.127	0.021
13	148.6	0.128	-0.064

Yaw damping results from the SHO Fit and Parameter ID methods are shown in Figures 5 and 6. Results from each run are presented as a symbol in the middle of a line. The line represents the approximate range of total yaw amplitude over the duration of a run, with the symbol marking the mid point of the line. The data are plotted at the mean values of C_{n_r} identified from the different data reduction methods. In general there is good agreement

Table 3: EEV Parameter ID Results

Run	q (Pa)	$C_{L_\beta}*$	C_{n_β}	C_{n_r}
07	43.7	0.224	0.186	-0.213
08	43.7	0.224	0.187	-0.341
09	43.9	0.224	0.182	-0.340
10	43.7	0.224	0.187	-0.281
11	96.4	0.224	0.183	-0.195
12	95.8	0.224	0.184	-0.215
13	95.9	0.224	0.185	-0.217
14	95.8	0.224	0.189	-0.297

$*$Assumed constant

Table 4: Stardust Parameter ID Results

Run	q (Pa)	C_{L_β}	C_{n_β}	C_{n_r}
02	105.2	0.907	0.125	-0.034
03	104.7	0.868	0.125	-0.019
04	104.8	0.775	0.126	-0.014
05	104.0	0.855	0.121	-0.093
06	152.7	0.909	0.124	-0.054
07	153.2	0.912	0.127	-0.065
08	153.2	0.934	0.123	-0.024
12	148.9	0.832	0.131	-0.056
13	148.6	0.816	0.129	-0.244

between the two methods. Both showing that the EEV model is dynamically stable ($C_{n_r} < 0$) and the Stardust model is near neutrally stable ($C_{n_r} \approx 0$). Note that all values from the Parameter ID method are less than zero. This is a limitation of the current implementation of the Parameter ID method; It currently assumes a damped system. Future work will modify the data reduction method to allow for undamped systems as well. The EEV data indicates that the Parameter ID method finds a more consistent and tighter cluster of results than the SHO-fit method, consistent with the methods ability to fully model the MSBS and aerodynamic forces and models.

The Stardust results from the Parameter ID method are all biased to be negative, while the SHO-fit method identified damping values that were near zero, but both positive and negative. The SHO-fit method identifies the yaw damping using an analytical solution to a simplified moment equation that includes the first order terms that affect capsule dynamics. The Parameter ID method uses a higher fidelity model to more fully reconstruct the position and attitude history and extracts force and moment coefficients. It is currently limited to damped vehicles, but future work will expand its capabilities. This comparison yields two important findings. First, the simple analytic solution describes the capsule motion very well, confirming that magnetic forces do not significantly corrupt capsule dynamics driven by the aerodynamic damping characteristics of a model. Second, the Parameter ID method is a robust and high fidelity tool that can extract static and dynamic forces and moments without the need for a priori estimates of the MSBS behavior or static aerodynamic characteristics of the model. More work remains, but this test established the Parameter ID method as our primary tool for the measurement of aerodynamics from free-to-oscillate testing in this magnetic suspension wind tunnel.

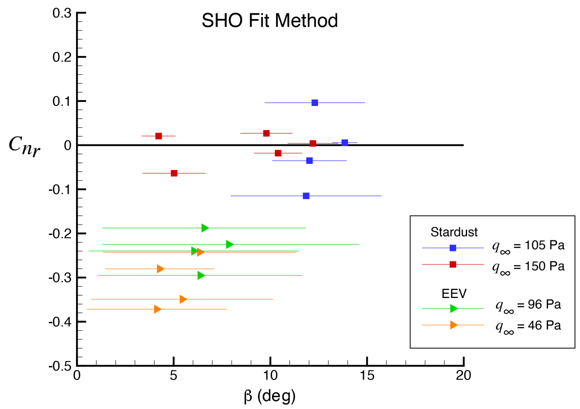

Fig. 5: SHO yaw damping results for all trials

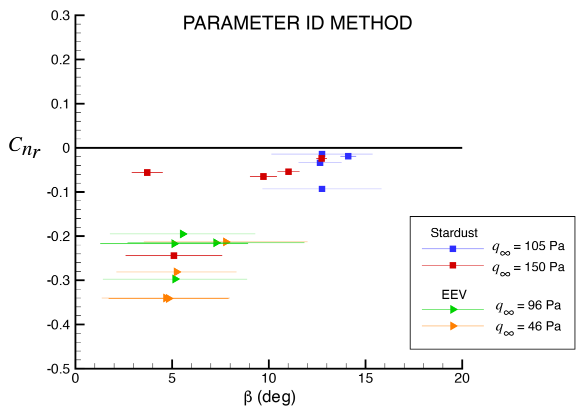

Fig. 6: SHO yaw damping results for all trials

6. Concluding Remarks

The data reduction development work combined with analysis of repeat runs has shown that the MIT/NASA/ODU subsonic magnetic suspension wind tunnel can be used to measure damping characteristics of blunt bodies. Fitting a SHO analytic solution provides reliable first order results, while a new Parameter ID method can separate aerodynamic and magnetic forces using an empirical characterization of the MSBS response in a wind-off configuration. Future work will further improve the Parameter ID method to measure dynamically unstable vehicles and add higher fidelity models to extract nonlinear damping curves.

References

[1] M. Schoenenberger, C. Finke, C. P. Britcher, D. Cox, *T.* Schott, *Static and Dynamic Testing of Blunt Bodies in a Subsonic Magnetic Suspension Wind Tunnel,* ICFD 2018, OS6-1, 2018.

[2] Q. McKown, M. Schoenenberger, D. Cox, *Uncertainty Analysis of the Pitch Damping Coefficient of Blunt Bodies, Measured from Magnetic Suspension Wind Tunnel Tests, ICFD 2020,* OS6-1, 2020.

[3] R. A. Mitcheltree, R. G. Wilmoth, F. M. Cheatwood, G. J. Brauckmann, F. A. Greene, *Aerodynamics of Stardust Sample Return Capsule,* JSR, Vol. 36, No. 3, May-June 1999.

[4] C. P. Britcher, M. Schoenenberger, D. Cox, *Demonstration of a Magnetic Suspension and Balance System with Transverse Magnetization,* ICFD 2019, OS6-1, 2019.